One-shot registration for crop recognition – Sentinel-2 and HySpex airborne images

Beata Hejmanowska, Piotr Kramarczyk, Rafał Zieliński

***Abstract*—The classification of agricultural land is important in many fields, including public administration, agriculture, forestry, and geography. We conducted research to analyze the possibility of using single remote sensing acquisition to determine land cover/use type on agricultural areas. Such a method is sometimes the only option in a moderate climate with a large number of cloudy days. We placed multitemporal satellite data based on Sentinel-2, as well as airborne data from the HySpex sensor, into Google Earth Engine - GEE. Additionally, we used an available automated method on GEE - Rapid Classification of Croplands, which we modified to local conditions. We performed Classification and Regression Trees, Random Forest, and Supported Vector Machine classification using reference data obtained in the field. The classification accuracy was respectively: 82% for the manually prepared Sentinel-2 time series, 75% for the single HySpex recording, and 65% for the automatically generated Rapid Season (6 seasons). The overall accuracy metric was used in the accuracy analysis. In the discussion, we referred to another metric commonly used in machine learning: accuracy, using which we could report an accuracy of >90%. All data and codes are available on Google Earth Engine.**

***Keywords* — Methodologies and Applications to Vegetation and Land Surface, Multispectral Data, Hyperspectral Data, Optical Data**

I. INTRODUCTION

Google Earth Engine (GEE) has revolutionized research areas utilizing remote sensing image processing. What used to take many days or weeks can now be accomplished in a matter of hours. Some tasks that are now possible using GEE were not possible before.

One critical area, particularly concerning food production safety, is crop monitoring. Recognizing crops using remote sensing has been the subject of research by many scientists for many years, such as yield forecasting [1.,2.], precision farming [3., 4.] and crop control [5.].

Regarding the use of GEE for this purpose, some example can be cited [6.]. Currently, machine learning methods such as Random Forest, Classification and Regression Trees (CART), Supported Vector Machine (SVM), and increasingly Deep Learning (DL) are used for crop recognition. The accuracy obtained varies depending on the type of crops, location, method, but mainly the preparation of training, validation, and testing data, accuracy metrics, and calculation methods [7.].

There are plenty examples of using only one reference set divided randomly or stratified on training and validation sample, while the distinction between training, validation and independent test data is extremely rare [8.].

Comparing different approaches is challenging because accuracies can be overestimated due to correlation between reference data in the training and validation sets [9., 14.]. Metrics for the testing sets are often not provided. Moreover, accuracy metrics are often referred to as accuracy ACC and presented as overall accuracy OA [13.].

Most researchers use Copernicus images: Sentinel-1 (S1) and Sentinel-2 (S2) for crop recognition. Unfortunately, in areas with a high number of cloudy days per year, it is difficult to obtain long time series with Sentinel-2. Therefore, an interesting approach is to use one-shot registration [10.,11.,12.].

In this article, we wanted to present the results of a study conducted using GEE on the reliability of crop recognition based on a single registration. We compared the results with the accuracy obtained from the time series created from Sentinel-2 images acquired from ESA Sentinel Open Hub and the Rapid Season method available in GEE (https://developers.google.com/). For comparison, due to the low spatial resolution, we used aerial images in addition to satellite data. We analyzed the accuracy using OA and in the discussion we referred to the ACC metric. Both of the above-mentioned issues are, in our opinion, the novelty of our research.

II. METHODS AND MATERIALS

A. Test area

Poland's agricultural landscape is characterized by large and regularly shaped fields in the North and center and smaller, elongated and irregular plots in the South. While S1/S2 imagery may be a suitable option for monitoring crops in the

This paragraph of the first footnote will contain the date on which you submitted your paper for review, which is populated by IEEE. It is IEEE style to display support information, including sponsor and financial support acknowledgment, here and not in an acknowledgment section at the end of the article. "This work was supported by program Excellence initiative—research university for the AGH University of Science and Technology no. 501.696.7996. The project title: Integration of remote sensing data for control in the system of direct agricultural subsidies (IACS)", *(Corresponding author: First A. Author).*

First A. Author is with the AGH University of Science and Technology / al. Mickiewicza 30, 30-059 Krakow, Poland (e-mail: galia@agh.edu.pl).

Second B. Author Author is with the AGH University of Science and Technology / al. Mickiewicza 30, 30-059 Krakow, Poland (e-mail: gorgany100@o2.pl).

Third C. Author is European Commission, Directorate General Joint Research Centre, Directorate for Sustainable Resources, Food Security Unit, Via E. Fermi 2749, I-21027 Ispra/Italy (e-mail: rafal.zielinski@gmail.com)

northern and central regions, it may present challenges for those in the southern areas.

To gather data on agricultural parcels that receive subsidies in Poland, a representative sample was selected in collaboration with the Agency for Restructuring and Modernisation of Agriculture (ARMA). The test area, situated near the town of Kolbuszowa, was chosen. ARMA provided information on approximately 5000 registered plots each year that receive subsidies. A majority of these parcels are small, with 75% of them measuring less than 1 hectare.

A. Data

When recognizing crops, the phenological stage of plants suitable for a given location should be taken into account. The entire phenological cycle of plants is usually analyzed during remote sensing crop recognition, if possible. In Poland, two seasons (the vegetative season and the dormant season), four periods (spring 100 days, summer 85 days, autumn 75 days, winter 105 days), and 12 phenological periods are distinguished (http://www.ogrody.orzysz.org.pl/ogrody/f_fenologia.htm).

The research period covered the year 2021. The data used in the experiment included: optical remote sensing data recorded from satellite and airborne platforms, other geospatial data, and reference data collected directly in the field.

The remote sensing data can be divided into three groups: all cloud-free scenes for the test area recorded by Sentinel-2, which were downloaded from the Sentinel Open Hub; Sentinel-2 collections available in GEE, which were used to generate composites according to the Rapid Classification of Croplands method (https://developers.google.com/); and hyperspectral images recorded from airborne platforms.

During the 2021 growing season, only six Sentinel-2 registration dates were cloud-free:

- S2B_MSIL2A_20210327T093039_N0214_R136_T34UEA_20210327T120034
- S2A_MSIL2A_20210411T093031_N0300_R136_T34UEA_20210411T122810
- S2B_MSIL2A_20210509T094029_N0300_R036_T34UEA_20210509T120133
- S2B_MSIL2A_20210725T093039_N0301_R136_T34UEA_20210725T115620
- S2B_MSIL2A_20210728T094029_N0301_R036_T34UEA_20210728T125908
- S2B_MSIL2A_20210906T094029_N0301_R036_T34UEA_20210906T113414

The Sentinel-2 images were acquired from Copernicus Open Access Hub as granules with a size of 100 per 100 km with a radiometric correction level of 2A in geographical coordinate system EPSG:4326. The images were not further corrected either geometric or radiometric. The pixel size depending on the channel is 10, 20 and 60m. A single S2 scene in SAFE (ESA) format takes approximately 1.2 gigabytes when packed.

The second satellite dataset consisted of composites created automatically in GEE using the function to remove cloud pixels from Sentinel-2 SR image (Composites for Crop Classification, End-to-End Google Earth Engine https://courses.spatialthoughts.com/end-to-end-gee.html) and seasonal composite creation. In the research, 3 and 6-season composites were analyzed.

Due to the high cost of aerial registration, it was only possible to make one hyperspectral registration. Based on our own experience and that of other researchers [10.], it was decided to date the registration approximately four weeks before harvest during the absence of cloud cover (July 5th, 2021). Hyperspectral data were acquired for the area ca. 5 x 4 km using HySpex VS-725 sensor which covers a very small area compared to the S2 range . The registration was performed at an altitude of 867 - 882 m. The HySpex VS-725 consists of two SWIR-384 scanners and one VNIR-1800 scanner which provide 430 spectral channels (414.13 nm - 2357.43 nm). The test area was covered with 16 strips. Radiometric, geometric (PARGE), atmospheric (ATCOR4) correction was performed using the MODTRAN physical model. The final product, an orthophotomap with a pixel size of 0.5 m was registered in the UTM 34N coordinate system (EPSG:32634) and takes up about 60 gigabytes.

Furthermore, ancillary geospatial data were acquired:

- Shuttle Radar Topography Mission - SRTM
- Archival topographic data from Central Geodetic and Cartographic Resource in Poland.

The DTM (Digital Terrain Model) and DSM (Digital Surface Model) were obtained from the national server: geoportal.gov.pl. Three DSM sheets (about 150 megabytes) and 15 DTM sheets (about 160 megabytes) with a pixel size of 1m.

A field visit on 7 July 2021 was conducted to obtain information about the ground truth (the plants grown in the parcels). Information in 56 agricultural plots was acquired by positioning the location using handheld GPS. In the field 10 agriculture land cover classes were found: beet, bare soils, barley, maize, oats, wheat rye, winter wheat, grass, potato and rye. Due to the single occurrence of some types of coverage, the following classes were selected for analysis: 2- bare soil, 5-oats, 6-wheat rye, 7-winter wheat, and 8-grass.

A. Data preprocessing

Based on the remote sensing images, the Normalized Vegetation Index (NDVI) was calculated for each date using the formula:

$$NDVI = \frac{NIR - R}{NIR + R} \qquad (1)$$

where:

- NIR - near infrared channel (Sentinel-2 - Band 8, HySpex - Band 136),
- R - red channel (Sentinel-2 - Band 4, HySpex - Band 81).

The slopes and exposures were calculated from the numerical terrain models (SRTM and DTM) using the Horn's algorithm [15.].

The image data, numerical terrain models and their derivatives

were merged using own code in Python as a stack and saved as a single tif file. Separately, one file from the Sentinel-2 time series, at 10 m resolution, and one file with hyperspectral data at 3 m resolution (the original HySpex 0.5 m data was resampled to 3 m).

There are 68 layers (bands) in the Sentinel-2 time series stack file. From 1-60 Sentinel-2 channels, 61 to 66 NDVI for each date (the channels used for calculation are also given), 67-68 DTM, aspect and slope.

There are 435 layers (bands) in the Hyperspectral stack file. From 1-430 HySpex channels, 431-434 DTM, DSM aspect and slope, 435 NDVI (the channels used for calculations are also given).

We also prepared a layer masking the area excluded from the analyses, a mask (of buildings and forests) using the k-means clustering method.

Three data sets are available on GEE:

- S2 stack https://code.earthengine.google.com/?asset=users/beatastark/stack_all
- HySpex stack https://code.earthengine.google.com/?asset=users/beatastark/mozaika_w_3m_ndvi_nmt_nmpt_slope_aspect
- mask https://code.earthengine.google.com/?asset=users/beatastark/maska_urban_forest_cluster

B. Methods

Two scripts were prepared for the study and made available in GEE: https://code.earthengine.google.com/?accept_repo=users/beatastark/cropsKolbuszowa2021.
The first: code 1 - "S2_HySpex_CART_RF_SVM" is for S2 stack and HySpex stack classification. Second: code 2 - "PL_phenology" is based on Rapid Classification of Croplands (https://developers.google.com/) and on Multi-temporal Composites for Crop Classification (End-to-End Google Earth Engine – https://courses.spatialthoughts.com/end-to-end-gee.html).

C. Code 1

Analysis using code "S2_HySpex_CART_RF_SVM" run as follows:

- loading data:
  - region of interest (roi)
  - training fields
  - test fields
  - S2_stack
  - mosaic_3m_all
  - mask
- visualization of true-color and false-color S2 (using first registration) and HySpex
- selection of data set for classification
- feature extraction from selected data set of training parcels
- train classifiers: CART, RF and SVM
- classification
- visualization: classification results, training, testing vectors and the mask
- export of the classification results
- calculate the training error matrix and accuracy
- feature extraction from selected data set of testing parcels
- calculate the validation error matrix and accuracy

D. Code 2

Analysis using code "PL_phenology" run as follows:

- loading data:
  - region of interest (roi)
  - training fields
  - test fields
  - mask
- setting the phenological seasons in Poland
- creation of different composites for each seasons
  - Rapid Classification of Croplands
- classification: CART, RF, SVM (feature extracting, classifier training, classification, accuracy analysis on training and test pixels)
- classification results - visualizations and export

E. Accuracy analysis

The classification results: CART, RF, SVM, can be saved to Google Drive. In addition, accuracy results are reported for the training set (validation accuracy) and the test set (classification accuracy): overall accuracy (OA), error matrix. They were used to calculate other accuracy metrics (Table III), where: TP – true positive, TN – true negative, FP – false positive, FN – false negative.

TABLE III. ACCURACY METRIC

Name	**Formula**
Producer accuracy (PA) Sensitivity True positive rate (TPR)	$\frac{TP}{TP+FN}$
Specificity True negative rate (TNR)	$\frac{TN}{TN+FP}$
User accuracy (UA) Precision Positive predictive value (PPV)	$\frac{TP}{TP+FP}$
Accuracy (ACC)	$\frac{TP+TN}{TP+TN+FP+FN}$
F1 score	$\frac{2TP}{2TP+FP+FN}$
Overall accuracy (OA) Percent of correct precision	$\frac{\sum_{i=1}^{n} TP_i}{\sum_{i=1}^{n} \left(TP_i+TN_i+FP_i+FN_i\right)}$

III. RESULTS

Code 1 – "S2_HySpex_CART_RF_SVM" allows for the CART, RF, and SVM classification prepared and placed in GEE satellite and airborne hyperspectral data using a training and test dataset. Code 2 - "PL_phenology" enables the CART, RF, and SVM classification of along with accuracy analysis for any location on Earth provided that the user imports their own training and test vectors and modifies the phenological seasons if necessary.

The sample classification results for the S2 and the HySpex stacks are shown in Fig. 1. The color legend used in the classification results is explained in Fig. 2, where built-up and forested areas are masked in black. The overall accuracy (OA) results for the classification are presented in Fig. 4. The highest accuracy was achieved for the S2 (1-66) with RF method (82%). The accuracy of the single Sentinel-2 registration was below 50% in all cases (not presented in Fig. 4). The accuracy of the single hyperspectral airborne registration with additional data (HySpex (1-435)) was 77% for CART method. The accuracy of the Rapid Classification of Croplands method was lower and the best result was achieved for 6 seasons using the SVM method (65%).

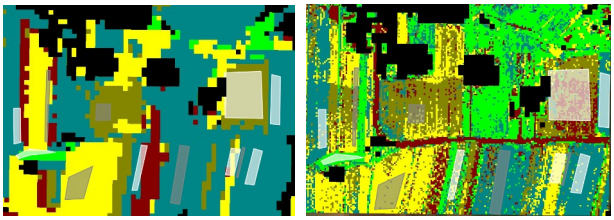

Fig. 1. Random Forest S2 (1-66 bands, pixel size 10m), HySpex (1-435 bands, pixel size 3m).

```
// Define a palette for the  classification.
var classPalette = [
  '#000000', // 1 not classified
  '#800000', // 2 barre soil
  '#000000', //3 not classified
  '#000000', // 4 not classified
  '#008080', // 5 oats
  '#FFFF00', // 6 wheat rye
  '#808000', // 7 wheat winter
  '#00FF00', // 8 grass
  '#000000', // 9 not classified
  '#000000', // 10 not classified

];
```

Fig. 3. Classification palette.

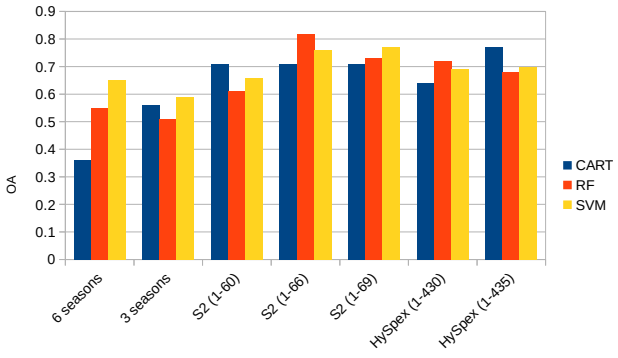

Fig. 4. Overall accuracy calculated using independent test data, in brackets bands used in classification.

III. DISCUSSION

In the discussion, we would like to refer to various accuracy metrics. All accuracy metrics listed in the Table III can be calculated based on the error matrix. An example error matrix for the best result obtained for the S2 (RF) and for HySpex (CART) is presented in Table IV. Accuracy metrics are presented in Tables V and VI. It is worth noting the comparison between OA and ACC, which differ significantly from each other. In the case of the S2 the OA accuracy is 82%, while the average ACC is 93%. For a single HySpex image, the difference is even greater, with an OA of 77% and an average ACC of 96%. We would like to highlight the importance of reporting how accuracy metrics are calculated. This is particularly important nowadays, when machine learning approaches are widely used, and ACC is often reported instead of OA. In Table IV and V, the corresponding accuracy metrics used in traditional remote sensing and machine learning are presented. In addition, a metric not used in remote sensing, specificity or true negative rate (TRN), is presented. TRN, like ACC, usually takes a very high value in multi-class classification due to the use of TN cases, which are normally very large in multi-class classification. Among the metrics used in machine learning, directly adapted from medical tests (two-class tests), such as sensitivity, specificity, and accuracy, only sensitivity has a counterpart in traditional remote sensing metrics. Sensitivity or true positive rate (TPR) is equal to the producer accuracy (PA).

TABLE IV. ERROR MATRIX (TEST SET)
LEFT – S2 (1-66 BANDS, RF), RIGHT - HYSPEX (1-435 BANDS, CART)

	ground true									
ID	**2**	**5**	**6**	**7**	**8**	**2**	**5**	**6**	**7**	**8**
2	3	6	24	0	0	239	22	62	0	61
5	0	52	0	0	0	0	707	17	9	12
6	2	6	28	2	0	7	36	76	289	14
7	4	8	0	70	0	73	83	68	764	0
8	0	0	0	0	88	0	31	10	0	927

TABLE V. METRICS S2 (1-66 BANDS, RF), **OA=0.82**

TPR/PA	TRN	PPV/UA	ACC	F1
0.33	0.89	0.09	0.88	0.14
0.72	1.00	1.00	0.93	0.84
0.54	0.96	0.74	0.88	0.62
0.97	0.95	0.85	0.95	0.91
1.00	1.00	1.00	1.00	1.00
0.71	**0.96**	**0.74**	**0.93**	**0.70**

TABLE VI. METRICS HYSPEX (1-435 BANDS, CART), **OA=0.77**

TPR/PA	TRN	PPV/UA	ACC	F1
0.75	0.95	0.62	0.94	0.68
0.80	0.99	0.95	0.94	0.87
0.33	0.89	0.18	0.86	0.23
0.72	0.91	0.77	0.85	0.75
0.91	**0.98**	**0.96**	**0.96**	**0.94**

IV. Conclusions

The selected test area was challenging, with a large number of cloudy days and a predominant number of small agricultural plots. Despite this, surprisingly good accuracy was achieved for Sentinel-2 time series, at 82%. On the other hand, the classification accuracy using a single hyperspectral airborne registration was surprisingly low at 77%. It should be noted that the accuracy was determined with respect to the so-called pixel-based approach. Additionally, the "salt and pepper" effect is visible, meaning that pixels belonging to different classes are present within one plot. This fact does not necessarily imply incorrect classification, but may reflect the real situation within one field (e.g., areas of bare soil, crops, weeds, etc.). The solution to this problem is an object-based approach, which will be the next stage of work.

The aim of the article was also to present different accuracy metrics to draw attention to the reliability of reported accuracy values. In our case, we could report accuracy of 93% for Sentinel-2 and 96% for HySpex if we were to use mean accuracy (ACC) as the metric.

References

1. J. Cao, H. Wang, J. Li, Q. Tian, and D. Niyogi, “Improving the Forecasting of Winter Wheat Yields in Northern China with Machine Learning–Dynamical Hybrid Subseasonal-to-Seasonal Ensemble Prediction,”*Remote Sensing*, vol. 14, no. 7, p. 1707, Apr. 2022, doi: 10.3390/rs14071707.
2. M. Ayub, N. A. Khan and R. Z. Haider, "Wheat Crop Field and Yield Prediction using Remote Sensing and Machine Learning," 2022 2nd International Conference on Artificial Intelligence (ICAI), Islamabad, Pakistan, 2022, pp. 158-164, doi: 10.1109/ICAI55435.2022.9773663.
3. E. Roma and P. Catania, “Precision Oliviculture: Research Topics, Challenges, and Opportunities—A Review,” Remote Sensing, vol. 14, no. 7, p. 1668, Mar. 2022, doi: 10.3390/rs14071668.
4. A. Bojeri, F. Melgani, G. Giannotta, G. Ristorto, G. Guglieri and J. M. Junior, "Automatic Crop Rows Segmentation for Multispectral Aerial Imagery,"2022 IEEE Mediterranean and Middle-East Geoscience and Remote Sensing Symposium (M2GARSS), Istanbul, Turkey, 2022, pp. 78-81, doi: 10.1109/M2GARSS52314.2022.9839867.
5. V. P. Gómez, V. Del Blanco Medina, J. L. Bengoa and D. A. Nafría García, "Accuracy Assessment of a 122 Classes Land Cover Map Based on Sentinel-2, Landsat 8 and Deimos-1 Images and Ancillary Data," IGARSS 2018 - 2018 IEEE International Geoscience and Remote Sensing Symposium, Valencia, Spain, 2018, pp. 5453-5456, doi: 10.1109/IGARSS.2018.8519262.
6. Y. Liu, Q. Yu, Q. Zhou, C. Wang, S. D. Bellingrath-Kimura and W. Wu, "Mapping the Complex Crop Rotation Systems in Southern China Considering Cropping Intensity, Crop Diversity, and Their Seasonal Dynamics," in IEEE Journal of Selected Topics in Applied Earth Observations and Remote Sensing, vol. 15, pp. 9584-9598, 2022, doi: 10.1109/JSTARS.2022.3218881.
7. S. V. Stehman, G. M. Foody, “Key issues in rigorous accuracy assessment of land cover products”, Remote Sensing of Environment, Volume 231, 2019, 111199, ISSN 0034-4257, https://doi.org/10.1016/j.rse.2019.05.018.
8. X. Hu, W. Yang, H. Wen, Y. Liu, and Y. Peng, “A Lightweight 1-D Convolution Augmented Transformer with Metric Learning for Hyperspectral Image Classification,” Sensors, vol. 21, no. 5, p. 1751, Mar. 2021, doi: 10.3390/s21051751.
9. G. Foody, “Impacts of Sample Design for Validation Data on the Accuracy of Feedforward Neural Network Classification,”Applied Sciences, vol. 7, no. 9, p. 888, Aug. 2017, doi: 10.3390/app7090888.
10. M. G. Maponya, A. van Niekerk, Z. E. Mashimbye, “Pre-harvest classification of crop types using a Sentinel-2 time-series and machine learning,” Computers and Electronics in Agriculture, vol. 169, 2020, doi:10.1016/j.compag.2019.105164.
11. M. Shiyao, X. Wang, X. Hu, C. Luo, Y. Zhong, “Deep learning-based crop mapping in the cloudy season using one-shot hyperspectral satellite imagery,” Computers and Electronics in Agriculture, vol. 186, 2023, doi:106188.10.1016/j.compag.2021.106188.
12. J. Tang, X. Zhang, Z. Chen, and Y. Bai, “Crop Identification and Analysis in Typical Cultivated Areas of Inner Mongolia with Single-Phase Sentinel-2 Images,”Sustainability, vol. 14, no. 19, p. 12789, Oct. 2022, doi: 10.3390/su141912789.
13. Y. Wu, P. Wu, Y. Wu, H. Yang, and B. Wang, “Remote Sensing Crop Recognition by Coupling Phenological Features and Off-Center Bayesian Deep Learning,”, Remote Sensing, vol. 15, no. 3, p. 674, Jan. 2023, doi: 10.3390/rs15030674.
14. H. Xue et al., “Object-Oriented Crop Classification Using Time Series Sentinel Images from Google Earth Engine,” Remote Sensing, vol. 15, no. 5, p. 1353, Feb. 2023, doi: 10.3390/rs15051353.
15. B. Horn, “Hill shading and the reflectance map,” Proceedings of the IEEE, vol. 69, 1981, doi: 10.1109/PROC.1981.11918.